

# Random location of Multiple Sparse Priors for solving the MEG/EEG inverse problem

José D. López<sup>1</sup>, Jairo J. Espinosa<sup>1</sup> and Gareth R. Barnes<sup>2</sup>

**Abstract**—MEG/EEG brain imaging has become an important tool in neuroimaging. Current techniques based in Bayesian approaches require an a-priori definition of patch locations on the cortical manifold. Too many patches results in a complex optimisation problem, too few an under sampling of the solution space. In this work random locations of the possible active regions of the brain are proposed to iteratively arrive at a solution. We use Bayesian model averaging to combine different possible solutions. The proposed methodology was tested with synthetic MEG datasets reducing the localisation error of the approaches based on fixed locations. Real data from a visual attention study was used for validation.

## I. INTRODUCTION

The reconstruction of three dimensional images of the brain activity based on MEG/EEG data has been for almost 20 years one of the most powerful tools in neuroimaging. Current algorithms based on the Bayesian framework have improved the solution of those static and deterministic approaches used in the 90's. The main idea of the Bayesian framework is that if the MEG/EEG inverse problem is ill-posed, i.e. there are infinite solutions for a single dataset; it is not possible to perfectly reconstruct the neural activity, but at least a probability distribution with a given degree of certainty can be provided.

Nowadays one of the most widely used brain imaging algorithms is the Multiple Sparse Priors (MSP) [1]. Its main characteristic is the use of a set of possible focal active patches of cortex as prior information to reconstruct the brain activity (sparse priors). These patches are weighted in order to determine how much information they provide to the final reconstruction, this is achieved with an iterative process called Restricted Maximum Likelihood, using the negative variational Free energy as cost function [2].

The default MSP algorithm uses a fixed set of patches distributed over the cortex, ideally these patches should cover the entire cortical surface, but this would be at the expense of prohibitively large computational load or simply too sensitive to the large number of sources for providing a reliable solution. This sparse sampling means that focal sources located far from patch centres will be inaccurately reconstructed.

In this work we introduce an improvement to reduce the localisation error caused by the fixed and sparsely located of

patches, by implementing a random iterative generation of patches, solving the inverse problem several times and then averaging all the solutions with Bayesian Model Averaging (BMA) [3].

The BMA averages the solution of several models based on their relative probability as approximated using Free energy, providing robustness to the solution that cannot be obtained just taking the average, or the most probable model. Given that each model (source reconstruction with a random location of patches) has a Free energy associated, the BMA is easy to implement and computationally feasible. Previous work has demonstrated the effectiveness of BMA in the MEG context [3], [4].

This manuscript proceeds as follows. In Section II the MEG/EEG brain imaging is presented as the Bayesian solution of an inverse problem. Then the MSP algorithm is explained and the random generation of patches is introduced, this section finishes with an explanation of BMA and its implementation. In Section III simulation results with noisy synthetic MEG data are presented, these datasets were generated using realistic head models computed with the SPM8 software package (<http://www.fil.ion.ucl.ac.uk/spm>). In Section IV the proposed methodology is validated with real MEG data; visual cortex activity is reconstructed using the proposed framework. Finally the results are discussed.

## II. THEORY

The estimation of cortical current flow from external electromagnetic measurements in MEG/EEG is known as the inverse problem. If one makes the assumption that current flow is due mainly to pyramidal neurons orientated perpendicular to the cortical surface the problem is simplified somewhat. The cortex is then populated with a grid of thousands of possible sources or current dipoles to characterise the neural activity. The measured data  $Y$  can then be expressed as

$$Y = LJ + \epsilon \quad (1)$$

Here, the propagation model of the head  $L$  relates a set  $J \in \mathbb{R}^{N_d \times N_n}$  of  $N_d$  current dipoles with the potentials  $Y \in \mathbb{R}^{N_c \times N_n}$  acquired with  $N_c$  sensors for  $N_n$  time samples. Sensor noise and uncertainty on the propagation model are represented by zero mean Gaussian noise  $\epsilon$  with covariance:  $\text{cov}(\epsilon) = \Sigma_\epsilon$ . The image of brain activity is generated by finding magnitudes of the current dipoles  $\hat{J}$  that best fits the data.

In the linear model of eq. (1) the lead field matrix  $L$  (propagation model) is non invertible because the dipoles outnumber the sensors ( $N_c \ll N_d$ ), then the reconstruction

<sup>1</sup>José D. López and Jairo J. Espinosa are with Mechatronics school, Universidad Nacional de Colombia sede Medellín, Medellín, Colombia. [jodlopezhi@unal.edu.co](mailto:jodlopezhi@unal.edu.co) - [jjespino@unal.edu.co](mailto:jjespino@unal.edu.co)

<sup>2</sup> Gareth R. Barnes is with Wellcome Trust Centre for Neuroimaging, University College London, London, United Kingdom. [g.barnes@ucl.ac.uk](mailto:g.barnes@ucl.ac.uk)

of the neural source activity  $\hat{J}$  cannot be directly recovered. This problem can be solved using the Bayesian framework by assuming a priori that  $J$  is a zero mean Gaussian process with covariance  $\text{cov}(J) = Q$ . The prior probability of the source activity  $p(J)$ , given by the previous knowledge of the behaviour of the brain; is corrected for fitting the data within the likelihood:  $p(Y|J)$ , allowing to estimate the source activity distribution using the Bayes' theorem:

$$p(J|Y) = \frac{p(Y|J)p(J)}{p(Y)} \quad (2)$$

The estimated magnitude of the current dipoles is recovered applying the expectation operator:  $\hat{J} = E[p(J|Y)]$ . Initially the evidence  $p(Y)$  is considered constant given that the dataset is fixed, but it will be introduced later in this manuscript to perform model selection.

The solution of eq. (2) is:

$$\hat{J} = QL^T(\Sigma_\epsilon + LQL^T)^{-1}Y \quad (3)$$

which is obtained with the argument that minimizes the gradient of eq. (2) with respect to the parameters  $J$  (See [5, Appendix] for four different ways to derive it). Finally, the posterior source covariance is given by:

$$\text{cov}(\hat{J}) = \Sigma_J = Q - QL^T(\Sigma_\epsilon + LQL^T)^{-1}LQ \quad (4)$$

In absence of information about the sensor noise, it is considered uniformly distributed and identically independent:  $\Sigma_\epsilon = \lambda_0 I_{N_c}$ , with  $I_{N_c} \in \mathfrak{R}^{N_c \times N_c}$  an identity matrix, and  $\lambda_0$  the sensor noise variance. This result provides enough information to solve the inverse problem under Gaussian assumptions for a known prior source covariance matrix  $Q$  (See [6] for a discussion about assuming the MEG/EEG inverse problem as a Gaussian process).

### A. Multiple Sparse Priors

The main characteristic of the Bayesian approach is the use of Empirical Bayes to form the source covariance matrix  $Q$  with a set of fixed covariance components  $C = \{C_1, \dots, C_{N_q}\}$  [7]:

$$Q = \sum_{i=1}^{N_q} e^{\lambda_i} C_i \quad (5)$$

Each of these components  $C_i$  is formed by a patch that represents a focal region of neural activity. In [8] a Green's function based on a graph Laplacian was proposed for generating the set of components. This forms a compact set of bell shaped patches of finite cortical extent. The estimation of source activity consists on weighting these hyperparameters  $\lambda = \{\lambda_1, \dots, \lambda_{N_q}\}$  for giving priority to those patches located in active regions.

1) *Optimisation process:* The optimisation of hyperparameters  $\lambda$  is performed with a non-linear search algorithm called Restricted Maximum Likelihood (ReML), that follows the gradient and curvature of the Free energy with respect to the hyperparameters [1]. The Free energy approximates the log of the model evidence  $F \approx \log p(Y)$ , when the source estimate  $\hat{J}$  approximates the truth.

For a given combination of hyperparameters the Free energy is expressed as [2]:

$$F = -\frac{N_c}{2} \text{trace} \left( \frac{\Sigma_Y}{\Sigma} \right) - \frac{N_c}{2} \log |\Sigma| - \frac{N_n}{2} \ln 2\pi + \frac{1}{2} (\mu - \nu)^T \Pi (\mu - \nu) + \frac{1}{2} \log |\Sigma_\lambda \Pi| \quad (6)$$

where  $|\cdot|$  is the matrix determinant operator,  $\Sigma_Y = \frac{1}{N_c} Y Y^T$  is the sample covariance matrix,  $\Sigma = \Sigma_\epsilon + LQL^T$  is the model based sample covariance matrix, and the prior and approximate densities of the hyperparameters are considered as Gaussian distributed:  $p(\lambda) = \mathcal{N}(\lambda; \nu, \Pi^{-1})$ , and  $q(\lambda) = \mathcal{N}(\lambda; \mu, \Sigma_\lambda)$  respectively. The optimal combination of hyperparameters is achieved for the maximum Free energy value:  $\hat{\lambda} = \arg \max_\lambda F$ , which is where the free energy is approximately equal to the log evidence.

2) *Random generation of patches:* Given that the posterior is Gaussian, the optimisation with ReML guarantees convergence. At this point we make two assumptions: First, those patches near to a true (but missing) source will have higher hyperparameter values. Second, a MSP reconstruction based on a set of patches that include the true source location, will have higher Free energy than a reconstruction which does not.

The default MSP generation of patches is performed as follows: Initially a Green's function  $Q_G \in \mathfrak{R}^{N_d \times N_d}$  is generated for all the  $N_d$  available dipoles. Then a set of  $N_q < N_d$  dipoles are selected guaranteeing that they are distributed over the entire cortical surface. Finally, each diagonal matrix  $C_i$  is formed with the column of  $Q_G$  that corresponds to one of the  $N_q$  dipoles previously selected.

The proposed method consists in modifying the way that the set of  $N_q$  dipoles is selected, by choosing randomly the location of the patches and performing several reconstructions for guaranteeing that the true source location is included. Finally, a BMA is performed for averaging all solutions based on their Free energy in order to obtain robust neural source estimation. In the following section the method will be explained step by step.

### B. Bayesian Model Averaging

One advantage of using ReML is that each source reconstruction is associated to a Free energy value, i.e. several reconstructions may be compared and the one with higher Free energy will be the most likely, because it is the most approximated to the evidence  $p(Y)$ . However, when several reconstructions have similar Free energy values selecting just one may not be the best option; besides that, averaging them based on their own probability adds robustness to the solution.

Let define  $B \in \mathfrak{R}^{N_b \times 1}$  as a set of  $N_b$  source reconstructions, each with its own estimation  $\hat{J}_i$  computed with eq. (3), covariance  $(\Sigma_J)_i$  computed with eq. (4), and Free energy  $F_i$  obtained in the ReML obtimisation, for  $i = 1, \dots, N_b$ . This forms the probability distributions of obtaining the true source estimates with a given model  $B_i$ :  $p(J|Y, B_i)$ . The

BMA provides a robust average of these  $B_i$  models based on their own probability:

$$p(J|Y) = \sum_{i=1}^{N_b} p(J|Y, B_i)p(B_i|Y) \quad (7)$$

where  $p(B_i|Y)$  is the probability of the model being true, fitted with the dataset  $Y$ . But given that  $Y$  is the same for all  $N_b$  models, this probability can be indirectly computed with:

$$p(B_i|Y) \approx \exp(F_i - \bar{F}) \quad (8)$$

with  $\bar{F}$  the mean Free energy over the  $N_b$  models, and  $F_i$  the free energy of the  $i$ -th model. The posterior probability distribution  $p(B|Y)$  must be normalised for guaranteeing that the total probability is 1.

The following algorithm is used to provide an estimate of  $\hat{J}$ , performed over  $T = 10000$  iterations and  $N_b = 1000$  models:

---

a) Perform  $N_b$  solutions for different randomly located patches and generate  $p(B|Y)$  with their Free energy values for  $t=1, \dots, T$  do

- b) Pick a solution from its posterior probability distribution:  $B_k \sim p(B|Y)$
  - c) For the solution  $B_k$  obtain the estimated values  $\hat{J}_k$  and their posterior covariance  $(\Sigma_J)_k$
  - d) Obtain a normal random variable with mean  $\hat{J}_k$  and covariance  $(\Sigma_J)_k$ :  $\tilde{J}_t \sim \mathcal{N}(\hat{J}_k, (\Sigma_J)_k)$ . In practice, for computational efficiency and storage limitations only the main diagonal of each  $(\Sigma_J)_k$  is computed in eq. (4)
- end for**

- Obtain the mean of the random variables:  $\hat{J} = \sum_t \tilde{J}_t$

---

Step (a) comprises  $N_b$  solutions of the inverse problem each with a random set of patches; this step is the only one computationally intensive and must be optimised in future works (each inversion takes around 30 seconds in a desktop computer). The BMA steps are computationally very efficient, on a desktop computer it takes less than one minute.

### III. SIMULATION RESULTS

Several simulations with different number of sources were performed to test the approach. For each test a single trial dataset of  $N_n = 161$  samples over  $N_c = 274$  MEG sensors was generated by projecting a known neural source distribution into sensor space. These neural sources consisted on pure sinusoidal signals. Gaussian white noise was added to the data to give a sensor level Signal to Noise Ratio ( $SNR$ ) of zero decibels (same signal and noise power). Figure 1(a) shows an example of a source located intentionally far from the nearest patch, Figure 1(b) shows the default MSP estimation with a fixed set of patches, all patches were spatially normally distributed with full width half maximum of approximately 10 mm. Due to the absence of patches at the simulated source location, two nearby regions were activated

causing a localisation error of 9.77 mm. The translucent glass brains of Figure 1 show the frontal, lateral and superior views of the 512 sources with highest variance during the time windows of interest.

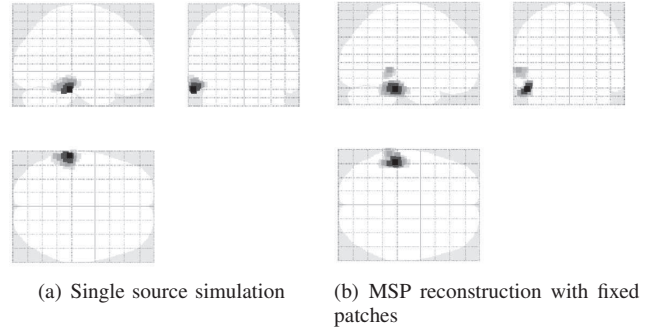


Fig. 1. Glass brains with frontal, lateral and superior views of the power of the neural activity: 1(a) Source generated intentionally far from the nearest patches. 1(b) MSP reconstruction with a fixed set of patches, the localisation error was 9.77 mm and the activity was divided in two regions.

Figure 2(a) shows the Free energy values of  $N_g = 1000$  reconstructions, Most of them had high values showing the capability of MSP to generate adequate solutions. Figure 2(b) shows the sorted probability of all 1000 models, the top 5 % of most probable models was achieved with just the first two models, and the 95 % cumulative probability distribution (CDF) is achieved with the first 162 models. The bottom 5 % of most probable models (838 models) were not included in the BMA. Figure 2(c) shows the BMA estimation of the neural activity map, the localisation error was zero and the solution was almost the same of the original map (Figure 1(a)). The robustness in the solution is evidenced in Figure 2(d), where the map of the worst solution in terms of Free energy ( $F = 2304.8$ ) effectively presented several ghost sources rounding the true active region.

After several tests (10 in total with up to 3 sources randomly located) the default MSP solution presented a mean localisation error of 8.74 mm, while the proposed approach presented a mean localisation error of 1.48 mm. The MSP presented rare cases of up to 50 mm of localisation error (especially with deep sources), but all solutions with the proposed approach presented maximum localisation errors of up to 10 mm.

Computationally the proposed approach took around 8 hours in a 2.4 GHz Intel Core i7 processor, with 6 GB RAM; which is too large compared with the approximately 30 seconds of the default MSP. However the provided robustness makes this time consumption feasible in neuroimaging; and it is expected that with parallel computing this time will be severely reduced because the iterations do not share information.

### IV. VALIDATION WITH REAL DATA

We used some MEG data acquired in a visual attention task to validate the method. A detailed description of the experimental set-up and previous data analysis were presented

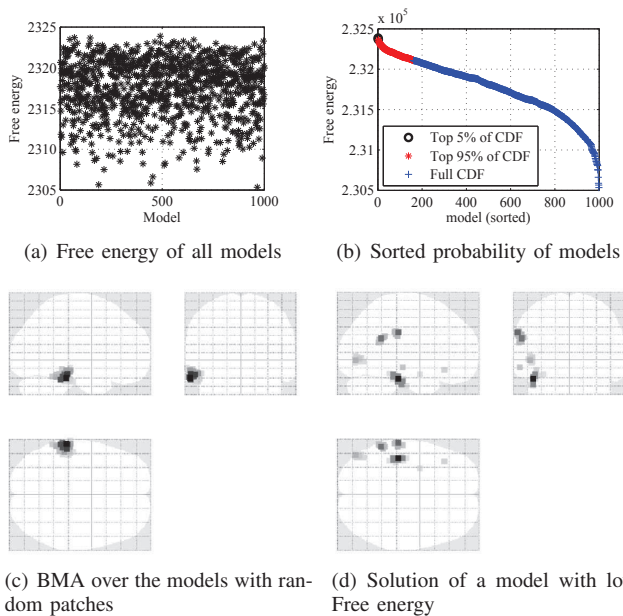


Fig. 2. 2(a) Free energy over  $N_g = 1000$  solutions, most of them have acceptable values. 2(b) Models within 95 % higher probability were used for BMA computation. 2(c) BMA reconstruction, the source was located with zero localisation error. 2(d) Example of a bad source reconstruction, several ghost sources appeared rounding the activation region.

in [9]. For this validation averaged single subject data were used.

Figure 3(a) shows the BMA estimate over  $N_b = 1000$  solutions with random patches, physiologically plausible sources in visual cortex can be observed and non interesting activity in other regions of the brain did not affected the reconstruction. Different case is shown in Figure 3(b), the source activity map of the reconstruction with lower Free energy demonstrates the problem of not having patches in the region of interest. All the activity was dispersed around the visual cortex, confirming both assumptions proposed before: Bad source reconstructions concentrate their activity in the patches nearer to the true neural source, and the Free energy values of bad reconstructions are lower than those with patches correctly placed. Here higher Free energy values rounded  $F = 1760$ , while the solution of 3(b) had a Free energy of  $F = 1754$ . A Free energy difference of 3 means that the solution is out of the 95 % of confidence interval; here the difference was 6, i.e. the probability of the worst model being the true one compared with the model of higher Free energy is 0.33 %.

Based on those results presented in this manuscript plus previous results (not shown here) valid reconstructions (based on Free energy, as shown on Figure 2(b)) were achieved in about 20 to 50 % of the iterations. Here a magic number of  $N_g = 1000$  iterations was used for demonstrating the concept, but statistically stable results can be achieved with  $N_g > 10$  (1 of every 10 simulations gives a feasible result), but for improving the mean error of the MSP this number must be considerably higher (at least  $N_g > 100$ ).

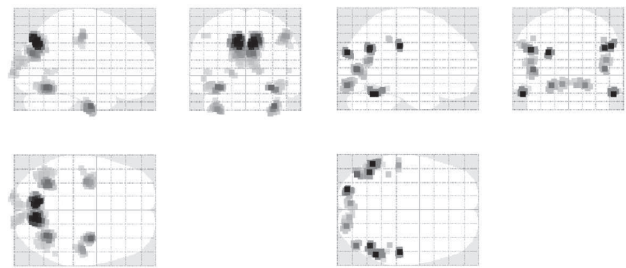


Fig. 3. 3(a) The BMA estimate recovered activity within the visual cortex coincident with previous analysis. 3(b) A bad location of sources caused also lower Free energy and a wrong brain image.

## V. CONCLUSIONS

In this manuscript a localisation improvement on the MSP inversion scheme was presented, it was shown how averaging the brain images of several solutions based on random location of patches, reduced the localisation error and added robustness to the solution.

We have demonstrated a robust and generic scheme which could be extended to address question of patch extent or even, given accurate knowledge of head location, possibly cortical layer.

## ACKNOWLEDGMENT

J.D. López and J.J. Espinosa are supported by ARTICA Research Centre for Excellence, Universidad Nacional de Colombia, and Colciencias, in the project “Procesamiento de Señales”. The Wellcome Trust Centre for Neuroimaging is supported by a strategic award from the Wellcome Trust. The authors would like to thank Marcus Bauer for providing the dataset and helpful information for this work.

## REFERENCES

- [1] K. Friston, L. Harrison, J. Daunizeau, S. Kiebel, C. Phillips, N. Trujillo-Barreto, R. Henson, G. Flandin, and J. Mattout, “Multiple sparse priors for the M/EEG inverse problem,” *NeuroImage*, vol. 39, pp. 1104–1120, 2008.
- [2] K. Friston, J. Mattout, N. Trujillo-Barreto, J. Ashburner, and W. Penny, “Variational free energy and the laplace approximation,” *NeuroImage*, vol. 34, pp. 220–234, 2007.
- [3] N. J. Trujillo-Barreto, E. Aubert-Vazquez, and P. A. Valdes-Sosa, “Bayesian model averaging in EEG/MEG imaging,” *NeuroImage*, vol. 21, pp. 1300–1319, 2004.
- [4] J. D. López, W. D. Penny, J. J. Espinosa, and G. R. Barnes, “A general Bayesian treatment for MEG source reconstruction incorporating lead field uncertainty,” *NeuroImage*, vol. 60, pp. 1194–1204, 2012.
- [5] A. K. Liu, A. M. Dale, and J. W. Belliveau, “Monte carlo simulation studies of EEG and MEG localization accuracy,” *Human Brain Mapping*, vol. 16, pp. 47–62, 2002.
- [6] J. D. López, “MEG/EEG brain imaging based on bayesian algorithms for ill-posed inverse problems,” Ph.D. dissertation, Universidad Nacional de Colombia, 2012 (Under review).
- [7] D. Wipf and S. Nagarajan, “A unified bayesian framework for MEG/EEG source imaging,” *NeuroImage*, vol. 44, pp. 947–966, 2009.
- [8] L. Harrison, W. Penny, J. Ashburner, N. Trujillo-Barreto, and K. Friston, “Diffusion-based spatial priors for imaging,” *NeuroImage*, vol. 38, pp. 677–695, 2007.
- [9] M. Bauer, C. Kluge, D. Bach, D. Bradbury, H. Jochen Heinze, R. J. Dolan, and J. Driver, “Cholinergic enhancement of visual attention and neural oscillations in the human brain,” *Current Biology*, 2012.